

Communication: Dynamical and structural analyses of solid hydrogen under vapor pressure

Kim Hyeon-Deuk and Koji Ando

Citation: *The Journal of Chemical Physics* **143**, 171102 (2015); doi: 10.1063/1.4935509View online: <http://dx.doi.org/10.1063/1.4935509>View Table of Contents: <http://scitation.aip.org/content/aip/journal/jcp/143/17?ver=pdfcov>Published by the **AIP Publishing**

Articles you may be interested in[On the room-temperature phase diagram of high pressure hydrogen: An ab initio molecular dynamics perspective and a diffusion Monte Carlo study](#)*J. Chem. Phys.* **141**, 024501 (2014); 10.1063/1.4886075[Hydrogen at extreme pressures \(Review Article\)](#)*Low Temp. Phys.* **39**, 402 (2013); 10.1063/1.4807051[Sound velocities in solid hydrogen under pressure](#)*Low Temp. Phys.* **39**, 423 (2013); 10.1063/1.4807043[Ortho-para conversion in the solid hydrogens at high pressures](#)*Low Temp. Phys.* **29**, 703 (2003); 10.1063/1.1614172[Impurity rotations in quantum versus classical solids: O₂ in solid hydrogens](#)*J. Chem. Phys.* **107**, 1544 (1997); 10.1063/1.474507



NEW Special Topic Sections

NOW ONLINE
Lithium Niobate Properties and Applications:
Reviews of Emerging Trends

AIP Applied Physics
Reviews

Communication: Dynamical and structural analyses of solid hydrogen under vapor pressure

Kim Hyeon-Deuk^{1,2,a)} and Koji Ando¹

¹Department of Chemistry, Kyoto University, Kyoto 606-8502, Japan

²Japan Science and Technology Agency, PRESTO, 4-1-8 Honcho, Kawaguchi, Saitama 332-0012, Japan

(Received 21 September 2015; accepted 29 October 2015; published online 5 November 2015)

Nuclear quantum effects play a dominant role in determining the phase diagram of H₂. With a recently developed quantum molecular dynamics simulation method, we examine dynamical and structural characters of solid H₂ under vapor pressure, demonstrating the difference from liquid and high-pressure solid H₂. While stable hexagonal close-packed lattice structures are reproduced with reasonable lattice phonon frequencies, the most stable adjacent configuration exhibits a zigzag structure, in contrast with the T-shape liquid configuration. The periodic angular distributions of H₂ molecules indicate that molecules are not a completely free rotor in the vapor-pressure solid reflecting asymmetric potentials from surrounding molecules on adjacent lattice sites. Discrete jumps of librational and H–H vibrational frequencies as well as H–H bond length caused by structural rearrangements under vapor pressure effectively discriminate the liquid and solid phases. The obtained dynamical and structural information of the vapor-pressure H₂ solid will be useful in monitoring thermodynamic states of condensed hydrogens. © 2015 AIP Publishing LLC. [<http://dx.doi.org/10.1063/1.4935509>]

Solid hydrogen is known as a typical quantum material in which each molecule exhibits large zero-point energy and nuclear delocalization.^{1–5} The solid-hydrogen phase diagram is greatly modified by accounting for such nuclear quantum effects (NQE).^{6–9} This typical quantum solid has actually attracted a number of theoretical and experimental researchers who adopted Raman scattering,^{10,11} neutron scattering,^{12–14} optical Kerr effects,¹⁵ lattice dynamics calculations,^{16,17} and path integral molecular dynamics (PIMD) simulations based on *ab initio* electronic potentials^{6–9,18} or spherical Silvera-Goldman (SG) model potentials.¹⁹

Pressure-induced structural changes have been reported by a combination of synchrotron experiments and density functional theory (DFT)-based PIMD calculations.^{6–10,20} The hexagonal close-packed (h.c.p.) structure is stable under relatively low external pressure, while pressure-induced orientational ordering accompanying a solid-solid phase transition was reported. Validity of the DFT descriptions in terms of an effective hydrogen interaction is however limited to very high density or pressure since most DFTs neglect the long-range dispersion interaction.^{18,21–23} The dispersion interaction is empirically included in the spherical SG model or in Lennard-Jones model potentials,²⁴ but its transferability to different phases is not obvious.¹⁹ Additionally, these PIMD simulation methods are appropriate for ensemble averages but not for real-time dynamics of each molecule.^{3–5} In these senses, solid H₂ under vapor pressure still remains open for further investigations.¹¹

We recently proposed a simulation method of nuclear and electron wave packet molecular dynamics (NEWPMD) based on non-empirical *ab initio* intra- and inter-molecular interactions of non-spherical hydrogen molecules where

important NQEs of a hydrogen nucleus are non-perturbatively taken into account.^{25–27} It reproduces the long-range dispersion interaction depending on an intermolecular angle and thus gives the correct structures and transport properties such as diffusion coefficients and viscosities of liquid H₂ under vapor pressure without any empirical parameters.^{25,26}

This paper reports the first study with the NEWPMD method on real-time dynamics of low-pressure H₂ molecular solids. We provide intuitive understandings of real-time dynamics of each H₂ molecule including its angular and intramolecular degrees of freedom as well as asymmetric lattice phonon modes which are intrinsic to solid H₂ under vapor pressure.

The NEWPMD approach describes nuclei by floating and breathing Gaussian WPs via the time-dependent Hartree approach, and EWPs by the perfect-pairing valence bond theory that appropriately treats the Pauli exclusion energy and intermolecular dispersion energy.^{25–27} It is thus distinguished from most of the previous nuclear wave packet (NWP) approaches in which a potential surface was given in advance by a separate modeling and, in many cases, expanded quadratically around the moving NWP centers to perturbatively take into account the NQEs.^{28–37} We set up 211 H₂ molecules at the saturated vapor pressure; the molar volume, $23.06 \times 10^{-6} \text{ m}^3/\text{mol}$, is taken from the saturated vapor pressure line at temperature ranging from 2.5 K to 13 K.¹ In cooling and equilibration runs started from the initial h.c.p. structure with randomly oriented H₂ molecules, atomic center momentum degrees of freedom are influenced by velocity scaling thermostat and Berendsen methods with each temperature. After the careful cooling and equilibration runs, we carried out NVE (microcanonical) simulations for 300 ps.

First visualization of dynamics in a solid state is given as real-time movies including H–H bond vibrations, molecular

^{a)}kim@kuchem.kyoto-u.ac.jp

orientations, and librational dynamics.³⁸ Throughout our 300 ps simulation, H₂ molecules maintain the h.c.p. lattice structure without any extra restriction on their molar coordinates. As shown in Fig. S1,³⁸ the mean square displacements almost linearly depending on the temperature indicate that each H₂ molecule stably oscillate around each lattice site without translational diffusion. The schematic h.c.p. lattice configuration is shown in Fig. 1(a). Figure 1(b) shows the two-dimensional (2D) radial distribution function (RDF) defined in Fig. S2³⁸ where the 2D RDFs at the other temperatures are provided. The first peak at $r = 3.8$ Å, which corresponds to a in Fig. 1(a), reflects nearest H₂ molecules on the same xy -plane and thus has a peak around $\cos \theta = 0$. However, the one-dimensional (1D) $\cos \theta$ -distributions have two split peaks just avoiding $\cos \theta = 0$ as in Fig. S3.³⁸ This contrasts with the H₂ liquid case where the θ -distribution has a broad peak around $\cos \theta = 0$,^{25,26} indicating that in the vapor pressure H₂ solid, most stable adjacent structure is not the T-shape as in the liquid case but the mutually deviated zigzag structure. The first peak is almost split into two peaks at 2.5 K reflecting the diatomic structure of nearest H₂ molecules (see also Fig. S4).³⁸ The split two peaks exhibit the similar distribution along the angular coordinate $\cos \theta$ in support of the stable and periodic molecular structure on the h.c.p. lattice. The similar angular distribution at the distance a is kept even at 13 K although the splitting of the first peak is smeared out reflecting enhanced orientational and lattice phonon motions at the higher temperature. In the liquid case, the angular fluctuation was smaller in the shoulder at the closer radial distance than in the main peak.²⁵

The second peaks on the $\cos \theta = -1$ and 1 lines correspond to second nearest H₂ molecules on the nearest xy -plane with the distance $r = \sqrt{2}a$; the second nearest H₂ molecules tend to be parallel to the central H₂ molecule. The radial distance where the third peak appears agrees with the distance from the second nearest xy -plane, c , in Fig. 1(a). The

angular distribution of this third peak is consistent with the zigzag configuration. The fourth peaks at 7.6 Å, i.e., $2a$, come from the second-nearest parallel configuration on the same xy -plane.

The solid 2D RDF exhibits the long-range periodic structure up to the fourth peak even at 13 K; the peaks and valleys of the solid 2D RDF become broader but are not deviated to larger distance nor broken. These are indicative of stable and periodic solidification of H₂ molecules, in contrast with the liquid case where the relative angle θ symmetrically distributed near 90° and the distribution became more uniform with larger radial distance.²⁵ The distribution along $\cos \theta$ is asymmetric in the solid 2D RDF. This asymmetric distribution stems from the non-uniform ordered zigzag structure of the solid crystal. In fact, we obtain the symmetric $\cos \theta$ -distributions by integrating the solid 2D RDF over the radial coordinate r as shown in Fig. S3.³⁸

2D angular distributions of ϕ_{xy} and ϕ_z at different temperatures are displayed in Fig. 1(c). The 2D distributions have periodic peaks at $\phi_{xy} = 30^\circ, 90^\circ$, and 150° . These constant 60° intervals as well as the periodic peaks around $\phi_z = 70^\circ$ and 110° indicate the periodic solid structure under vapor pressure. The long peaks along $\phi_z = 0^\circ$ and 180° indicate that H₂ molecules tend to align along z -axis. The other angular distributions are provided in Figs. S5 and S6.³⁸ The non-uniform distribution indicates that the H₂ molecules are not rotating freely but are under anisotropic molecular interaction on the h.c.p. lattice. Actually, the 2D RDFs of the H₂ liquid at higher temperature exhibit a peak around $\theta = 90^\circ$ in their first peak reflecting the most stable T-shape structure; the θ -distribution then becomes uniform with increasing the radial distance, which indicates that a H₂ molecule becomes free from the external potential.²⁵ The current periodic angular distributions of the H₂ solid demonstrate that the rotational order is relatively conspicuous all over the vapor-pressure solid. We emphasize that the

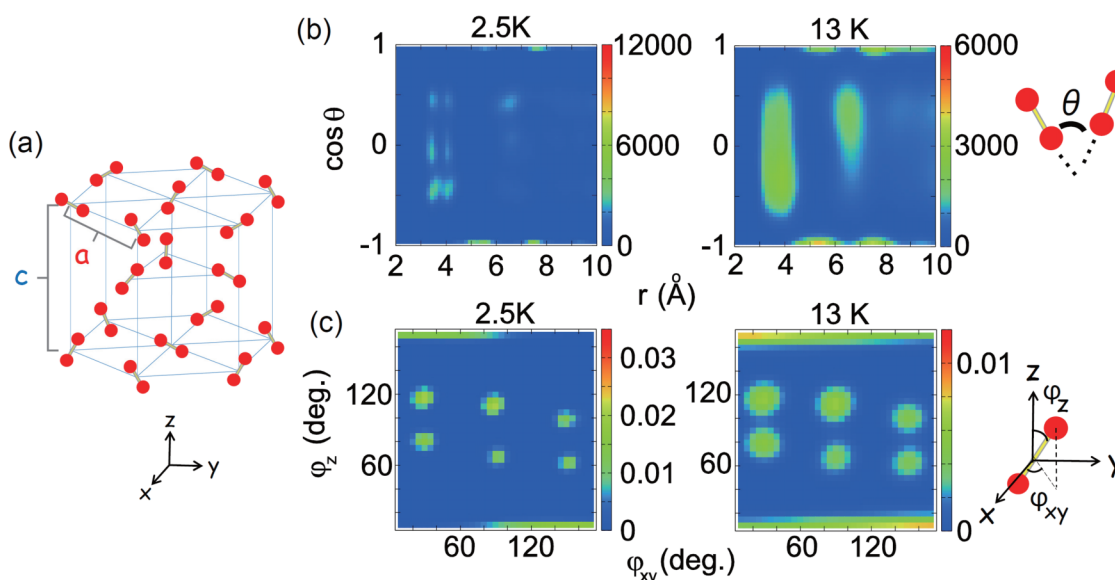


FIG. 1. (a) Schematic h.c.p. lattice structure of solid H₂ under vapor pressure, (b) 2D RDFs, and (c) 2D angular distributions at 2.5 K and 13 K. The 2D RDFs of solid H₂ exhibit long-range periodic structures. The most stable solid configuration of adjacent molecules is a zigzag structure and H₂ molecules in the vapor-pressure solid are not a completely free rotor.

current periodic angular distribution was naturally obtained from randomly oriented H_2 molecules on the initial h.c.p. lattice.

The phonon frequency of solid hydrogen is highly sensitive to pressure; the frequency shifts from 36 cm^{-1} for the vapor pressure solid to approximately 1000 cm^{-1} for a high-pressure solid at 150 GPa. The large frequency shift of phonon modes provides an important test of the current intermolecular potential including the attained pressure and indicates significant difference between the phonon dynamics under vapor pressure and high pressure.^{15,20,39} Figure 2(a) shows power spectra for real-time distance of each hydrogen atom in the space-fixed frame. At all the temperature, a peak around 40 cm^{-1} is observed, which is close to the experimental E_{2g} phonon mode frequency of 36 cm^{-1} for the vapor-pressure H_2 solid.²⁰ We assign this peak frequency, 40 cm^{-1} , to the phonon frequency of the current h.c.p. lattice because of the following features: (1) The peak intensity increases almost linearly depending on the temperature, which reflects temperature-dependent lattice phonon fluctuations. (2) The peak frequency is not red-shifted but maintains the frequency

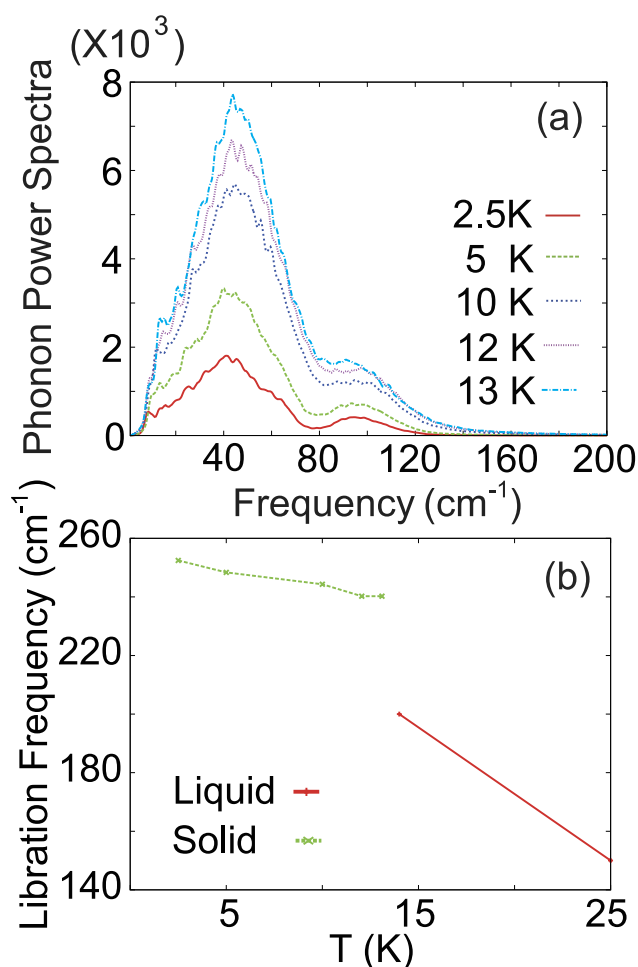


FIG. 2. (a) Phonon power spectra and (b) temperature dependence of librational frequency of the vapor-pressure H_2 solid. The lattice phonon peak frequency keeps 40 cm^{-1} while the librational frequency is sensitive to the temperature. The discrete jump of the librational frequency between 13 K and 14 K is rationalized by a drastic structural change at the liquid-solid phase transition.

of 40 cm^{-1} throughout all the temperatures, indicating stability of the lattice. (3) As in Fig. S7,³⁸ the spectral intensity of the z-coordinate is much larger than the intensity of the x- and y-coordinates, which originates from the asymmetric lattice phonon modes based on the asymmetric h.c.p. structure. (4) The peak of 40 cm^{-1} with features (1)–(3) was absent in liquid H_2 .²⁵ The high energy edge of the phonons up to mid- 100 cm^{-1} is also similar to the experimental observations of neutron scattering.^{12–14} The agreement with experiments of the phonon frequency, which is highly sensitive to external pressure, ensures that this simulation realized the vapor-pressure solid.

The power spectra for the real-time intermolecular angle $\theta(t)$ have the peaks of approximately 250 cm^{-1} which we assign to librations of H_2 molecules rather than to rotational motions (Figure S8).³⁸ As shown in Fig. 2(b), while the lattice phonon frequency is rather insensitive to the temperature, the redshift of the librational frequency reflecting softening of the local structure at the higher temperatures supports the current libration picture. Indeed, the temperature dependence of the librational frequency is more significant in the liquid cases at 14 K and 25 K where the larger changes of the local T-shape structure occur.²⁵ The largest frequency change, the discrete jump of the frequency between 13 K and 14 K, is rationalized by the drastic structural rearrangement and thus demonstrates the liquid-solid phase transition. The reasonable agreement with the experimental transition temperature endorses the accuracy of the intermolecular interactions. The above insights are further supported by the power spectra of the molecular angles in Fig. S5.³⁸

The H–H bond r_{HH} is significantly fluctuating depending on the temperature even in the vapor pressure solid H_2 and cannot be treated as a fixed bond as shown in Fig. S9(a).³⁸ The average H–H bond length at every temperature is summarized in Fig. 3(a). They all agree with the experimental data within an approximately 1% error.^{27,40} The average H–H bond length is longer at the lower temperature, which is nontrivial but agrees with the experimental finding in the vapor-pressure solid and liquid.⁴⁰ In the vapor-pressure solid, the H–H bond is effectively elongated by an attraction from an electron distribution in a bonding region of adjacent H_2 molecules as the crystal structure becomes more stiff. The larger rearrangement in local structures of the liquid than the solid rationalizes more significant temperature dependence of r_{HH} in the liquid. The discrete jump of the bond length between 13 K and 14 K again reflects the phase transition.

The H–H vibrational frequencies defined as the peak frequency of the power spectra in Fig. S9(b)³⁸ are summarized in Fig. 3(b). The H–H frequency is overestimated compared to the experimental data around 4149.6 cm^{-1} ^{1,10} by 11% that would be irrelevant to the discussions in this work. The H–H bond is stretched in the rigid structure at the lower temperature as discussed above, and, due to the resulting weakened bond potential, the vibrational frequency is red-shifted with decreasing the temperature. The calculated frequency jump caused by the phase transition is approximately 4 cm^{-1} which is close to the experimental frequency jump of 2 cm^{-1} .¹ This small change in the $4 \times 10^3\text{ cm}^{-1}$ of H–H vibrational frequency is reproduced with the combination of flexible electron and

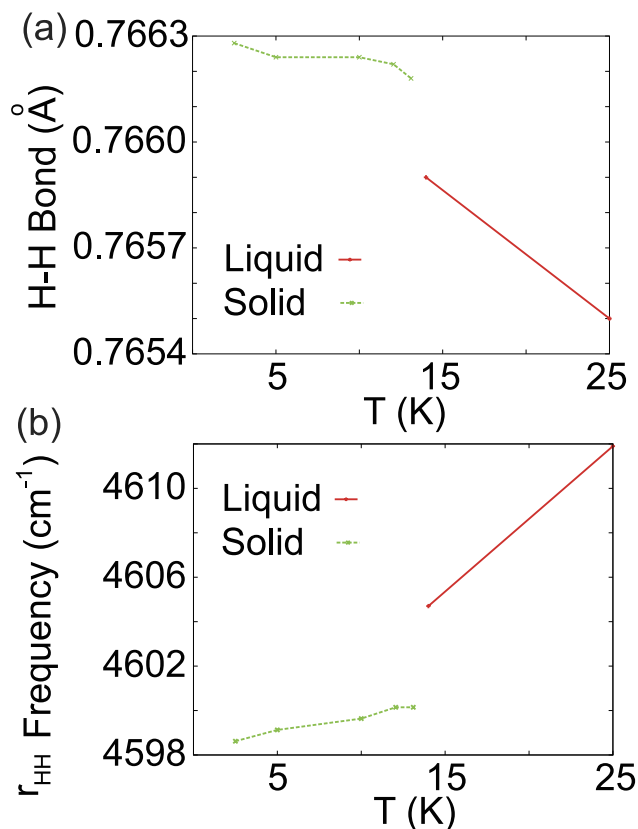


FIG. 3. Temperature-dependence of (a) average H-H bond length and (b) H-H vibrational frequency constituting the vapor-pressure solid H_2 . Higher condensation results in stretched H-H bond and thus in red-shifted H-H vibrational frequency. The discrete jumps between 13 K and 14 K distinguish the liquid and solid phases.

nuclear WPs.¹⁰ The less sensitive temperature dependence of the H-H vibrational frequency in the vapor-pressure solid than in the vapor-pressure liquid indicates smaller structural rearrangements in the stiff solid phase, being in agreement with the experimental tendency.¹ Analyses of the NWP beating motion anticorrelated to the H-H stretching mode are reported in Fig. S10.³⁸

This paper provided the dynamical and structural views of the low-pressure H_2 molecular solids with the real-time dynamics of each nonspherical H_2 molecule including its H-H bond vibrations, angular motions, NWP beatings, and phonon modes of the h.c.p. lattices. The discrete jumps of the librational frequency, average H-H bond length, and vibration frequency at the liquid-solid phase transition under vapor pressure are computationally found and analyzed in comparison with the vapor-pressure liquid and high-pressure solid.

The peak positions of the angular distribution such as the constant 60° intervals are in harmony with the high-pressure phase I solid.⁶ However, the current thermodynamic points, vapor pressure and temperatures below 25 K, are different from thermodynamics states where high-pressure phase I solids have been discussed. The present vapor-pressure H_2 solid simply connects to the vapor-pressure H_2 liquid: the blueshift of the H-H vibrational frequency with increasing the temperature simply links to the density decrease along the saturated vapor pressure line. The similar blueshift of the

H-H vibrational frequency was observed in the experiments on the vapor-pressure solids and liquids.¹ The high-pressure phase I solid exhibits the completely opposite tendency: the H-H bond length decreases with increasing the pressure up to 30 GPa, indicating simple compression of each hydrogen molecule.⁴⁰ The current H_2 molecules closely interacting each other on the h.c.p. lattice are not a free spherical molecule due to the asymmetric external interaction potential.

The insights obtained here suggest that solid-phase hydrogens constitute a new class of molecular quantum crystals even under vapor pressure that should be characterized by anisotropic molecules with angular and intramolecular degrees of freedom. Our work has initiated a quantitative trace of H_2 single molecule dynamics even in a solid phase and has wide scope for extensions in various thermodynamic phases including orientational ordering accompanying a phase transition.⁴¹ Directly obtained information on angular degrees of freedom and H-H vibrations as well as lattice phonon modes will play an essential role in monitoring thermodynamic states of condensed hydrogens.

K.H.D. thanks the financial supports from JST (PRESTO), Grant No. 10704, and Grant-in-Aids for Scientific Research from Japan Society for the Promotion of Science (KAKENHI), Grant No. 15K05386. K.A. acknowledges support from KAKENHI Nos. 26248009 and 26620007.

- ¹R. Sliter and A. F. Vilesov, *J. Chem. Phys.* **131**, 074502 (2009).
- ²M. E. Tuckerman, D. Marx, and M. Parrinello, *Nature* **417**, 925 (2002).
- ³G. Carleo, S. Moroni, and S. Baroni, *Phys. Rev. B* **80**, 094301 (2009).
- ⁴V. Sorkin, E. Polturak, and J. Adler, *J. Low Temp. Phys.* **143**, 141 (2006).
- ⁵V. Sorkin, E. Polturak, and J. Adler, *Phys. Rev. B* **71**, 214304 (2005).
- ⁶H. Kitamura, S. Tsuneyuki, T. Ogitsu, and T. Miyake, *Nature* **404**, 259 (2000).
- ⁷G. Geneste, M. Torrent, F. Bottin, and P. Loubeyre, *Phys. Rev. Lett.* **109**, 155303 (2012).
- ⁸C. J. Pickard and R. J. Needs, *Nat. Phys.* **3**, 473 (2007).
- ⁹S. Biermann, D. Hohl, and D. Marx, *Solid State Commun.* **108**, 337341 (1998).
- ¹⁰A. F. Goncharov, R. J. Hemley, H.-K. Mao, and J. Shu, *Phys. Rev. Lett.* **80**, 101 (1998).
- ¹¹M. Kuhnelt, J. M. Fernandez, G. Tejada, A. Kalinin, S. Montero, and R. E. Grisenti, *Phys. Rev. Lett.* **106**, 245301 (2011).
- ¹²A. Bickermann, H. Spitzer, H. Stiller, H. Meyer, R. Lechner, and F. Volino, *Z. Phys. B* **31**, 345 (1978).
- ¹³B. A. Vindryaevskii, S. N. Ishmayev, I. P. Sadikov, A. A. Chemyshey, Y. L. Shitikov, G. V. Kobelev, V. A. Sukhoparov, and A. S. Telepnev, *JETP Lett.* **62**, 822 (1995).
- ¹⁴S. Ishmaev, G. Kobelev, I. Sadikov, V. Sukhoparov, A. Chernyshov, A. Telepnev, B. A. Vindryaevskii, and Y. Shitikov, *Physica B* **234-236**, 30 (1997).
- ¹⁵F. Konigsmann, N. Schwentner, and D. T. Anderson, *Phys. Chem. Chem. Phys.* **15**, 17435 (2013).
- ¹⁶K. N. Klump, O. Schnepp, and L. H. Nosanow, *Phys. Rev. B* **1**, 2496 (1970).
- ¹⁷M. L. Klein and T. R. Koehler, *Phys. Lett. A* **33**, 253 (1970).
- ¹⁸K. Nagao, T. Takezawa, and H. Nagara, *Phys. Rev. B* **59**, 13741 (1999).
- ¹⁹H. Saito, H. Nagao, K. Nishikawa, and K. Kinugawa, *J. Chem. Phys.* **119**, 953 (2003).
- ²⁰H. Mao and R. J. Hemley, *Rev. Mod. Phys.* **66**, 671 (1994).
- ²¹J. M. McMahon, M. A. Morales, C. Pierleoni, and D. M. Ceperley, *Rev. Mod. Phys.* **84**, 1607 (2012).
- ²²K. Nagao, S. A. Bonev, A. Bergara, and N. W. Ashcroft, *Phys. Rev. Lett.* **90**, 035501 (2003).
- ²³M. Dion, H. Rydberg, E. Schroder, D. C. Langreth, and B. I. Lundqvist, *Phys. Rev. Lett.* **92**, 246401 (2004).
- ²⁴G. Garberoglio and J. K. Johnson, *ACS Nano* **4**, 1703 (2010).
- ²⁵K. Hyeon-Deuk and K. Ando, *Phys. Rev. B* **90**, 165132 (2014).

- ²⁶K. Hyeon-Deuk and K. Ando, *J. Chem. Phys.* **140**, 171101 (2014).
- ²⁷K. Hyeon-Deuk and K. Ando, *Chem. Phys. Lett.* **532**, 124 (2012).
- ²⁸F. Grossmann, *Chem. Phys. Lett.* **262**, 470 (1996).
- ²⁹F. Grossmann and T. Kramer, *J. Phys. A* **44**, 445309 (2011).
- ³⁰I. Georgescu, J. Deckman, L. J. Fredrickson, and V. A. Mandelshtam, *J. Chem. Phys.* **134**, 174109 (2011).
- ³¹E. Heatwole and O. V. Prezhdo, *J. Chem. Phys.* **126**, 204108 (2007).
- ³²S.-Y. Lee and E. J. Heller, *J. Chem. Phys.* **76**, 3035 (1982).
- ³³M. H. Beck, A. Jackle, G. A. Worth, and H.-D. Meyer, *Phys. Rep.* **324**, 1 (2000).
- ³⁴I. Burghardt, K. Giri, and G. A. Worth, *J. Chem. Phys.* **129**, 174104 (2008).
- ³⁵D. V. Shalashilin and M. S. Child, *J. Chem. Phys.* **128**, 054102 (2008).
- ³⁶K. Hyeon-Deuk and K. Ando, *J. Chem. Phys.* **131**, 064501 (2009).
- ³⁷K. Hyeon-Deuk and K. Ando, *J. Chem. Phys.* **132**, 164507 (2010).
- ³⁸See supplementary material at <http://dx.doi.org/10.1063/1.4935509> for real-time movies of solid p -H₂ at 2.5 K and at 13 K, and additional figures for intra- and inter-molecular structures and dynamics of the solid p -H₂ under vapor pressure.
- ³⁹R. J. Hemley and H.-K. Mao, *Elementary Processes in Dense Plasmas* (Addison-Wesley, Reading, 1995).
- ⁴⁰P. Loubeyre, M. Jean-Louis, and I. F. Silvera, *Phys. Rev. B* **43**, 10191 (1991).
- ⁴¹A. Driessen, E. van der Poll, and I. F. Silvera, *Phys. Rev. B* **30**, 2517 (1984).